Supporting Information

Laser-Irradiation Induced Synthesis of Spongy AuAgPt Alloy Nanospheres with High-index Facets, Rich Grain Boundaries and Subtle Lattice Distortion for Enhanced Electrocatalytic Activity

Tao Zhang, [ab] Yu Bai, [a] Yiqiang Sun, [ab] Lifeng Hang, [ab] Xinyang Li, [a] Dilong Liu,[a] Xianjun Lyu, [d] Cuncheng Li, [c] Weiping Cai, [a] Yue Li *[a]

a Key Laboratory of Materials Physics and Anhui Key Laboratory of Nanomaterials and Nanotechnology, Institute of Solid State Physics, Chinese Academy of Sciences, Hefei, 230031, China.

b University of Science and Technology of China, Hefei, 230026, P. R. China.

c Key Laboratory of Chemical Sensing & Analysis in Universities of Shandong (University of Jinan), School of Chemistry and Chemical Engineering, University of Jinan, Jinan, 250022, P. R. China

d Shandong University of Science and Technology, College of Chemical and Environmental Engineering, Qingdao, Shandong, China

*Email: yueli@issp.ac.cn

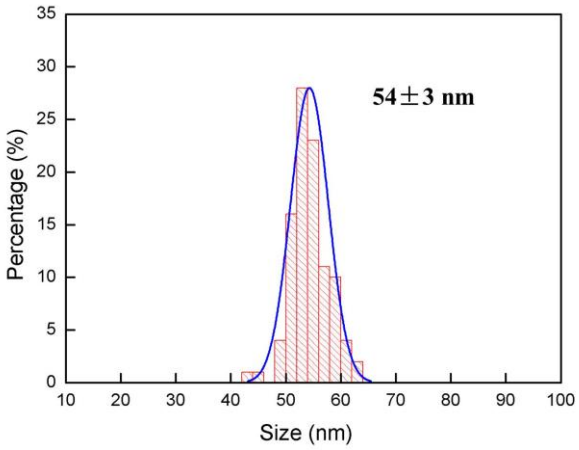

Fig. S1 Grain-size chart of the spongy AuAgPt alloy NSs.

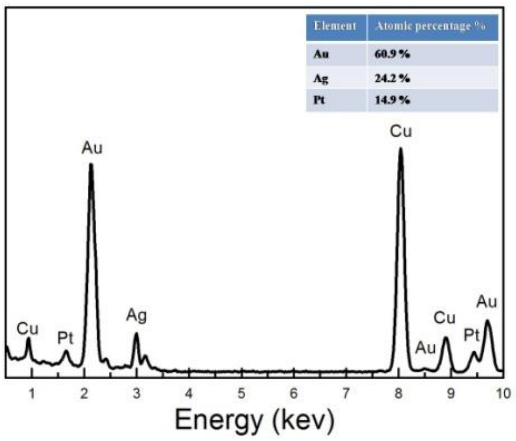

Fig. S2 EDS for spongy AuAgPt on the copper grid. The percentage of Au, Ag and Pt was 60.9%, 24.2% and 14.9%, respectively.

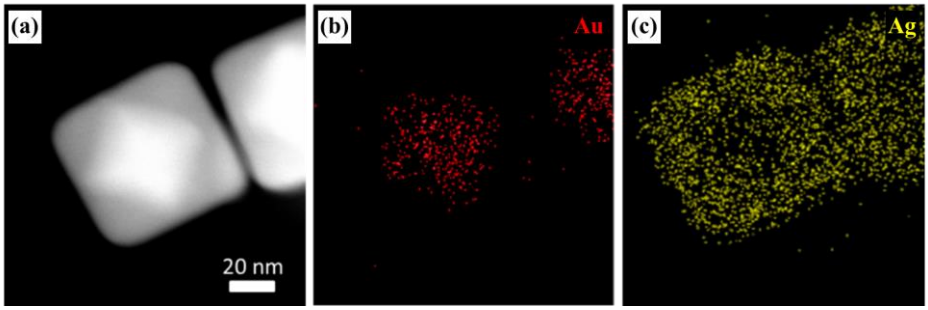

Fig. S3 HAADF-STEM image (a) and EDX elemental mapping (b, c) of Au@AgPt core-shell NCs.

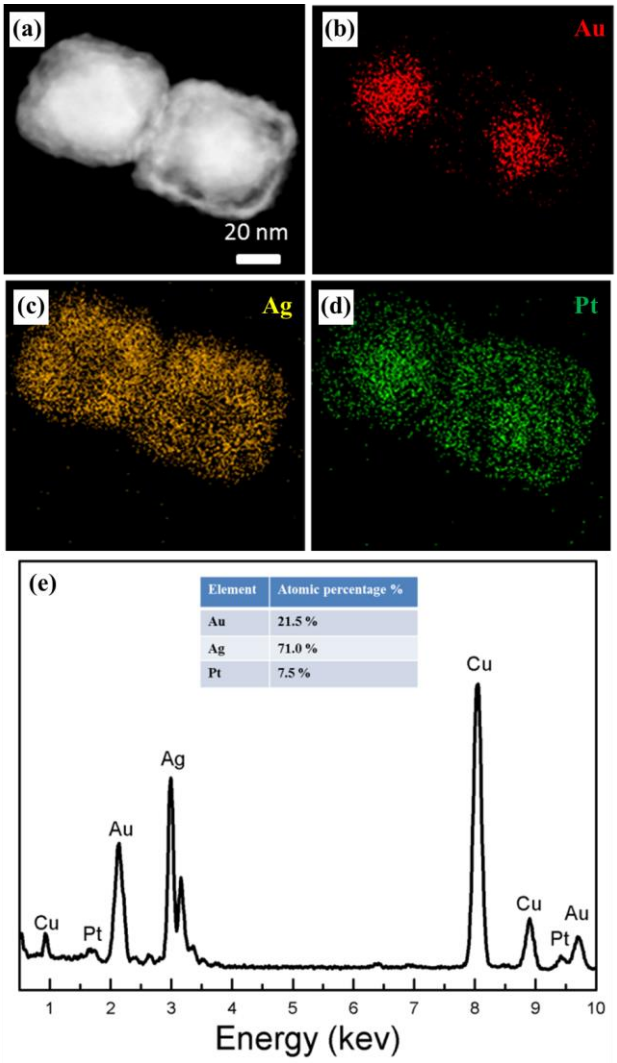

Fig. S4 HAADF-STEM image (a), EDS elemental mapping (b-d), and EDS (e) of Au@AgPt yolk-shell NCs.

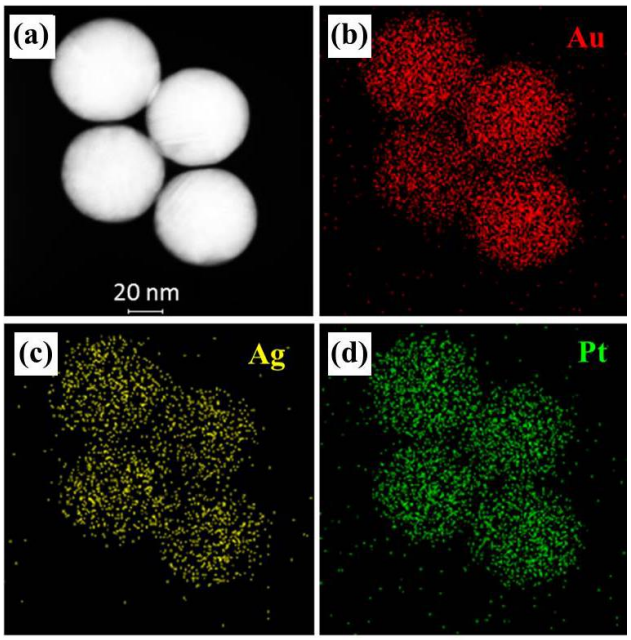

Fig. S5 HAADF-STEM image (a), EDS elemental mapping (b-d) of solid AuAgPt NSs.

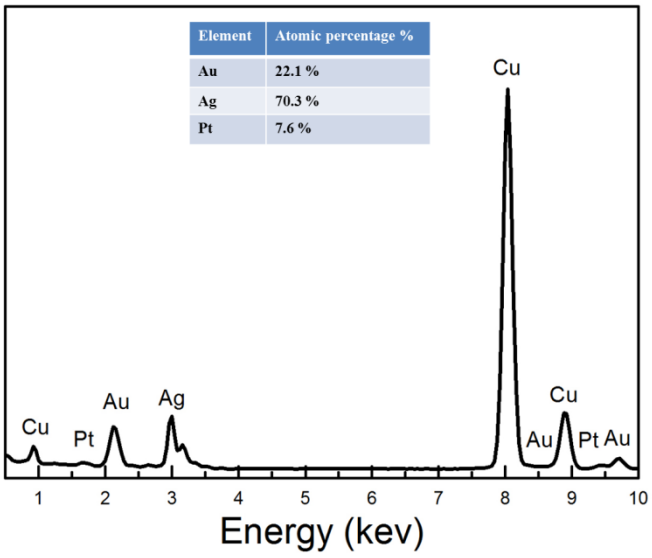

Fig. S6 EDS spectrum of the solid alloyed AuAgPt NSs.

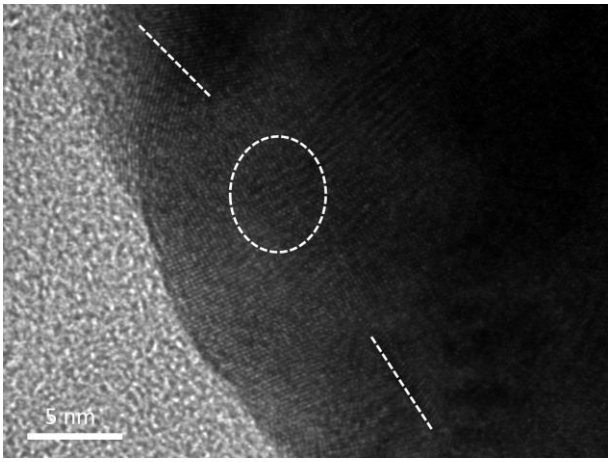

Fig. S7 HRTEM image of solid AuAgPt NSs. The grain boundaries were indicated by white dashed lines and lattice distortion was marked by white dashed circles.

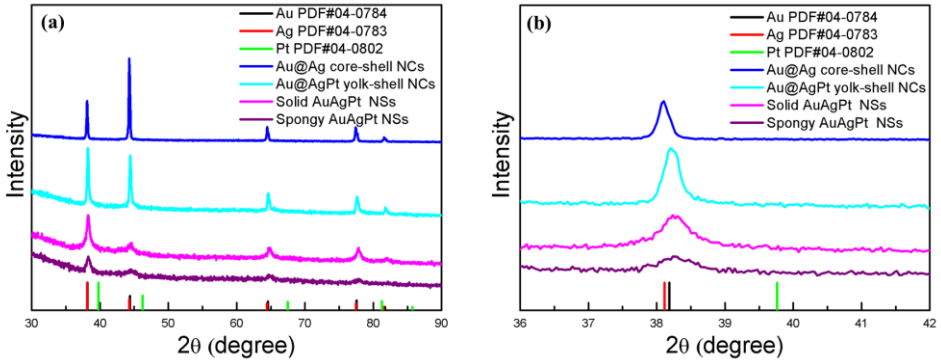

Fig. S8 PXRD patterns of Au@Ag core-shell NCs, Au@AgPt yolk-shell NCs, solid AuAgPt NSs, and spongy AuAgPt NSs together with the standard patterns for bulk Au, Ag, and Pt. The right one shows the diffraction peak (111) in the range of 36 to 42 degrees.

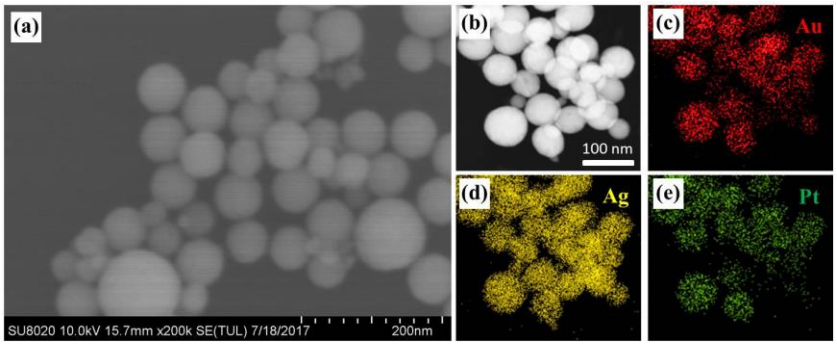

Fig. S9 FESEM (a), HAAD-STEM, and EDS elemental mapping (c-e) images alloyed NSs obtained at the high irradiation fluence of 14.65 mJ/cm^{-2}.

Table S1. MOR activities of various reported catalysts.

Catalysts	Mass activity (A/mg_{Pt})	Specific activity (mA/cm^2)	Electrolyte	References
S-AuAgPt NSs	**1.62**	**3.55**		**This work**
$PtCu_{2.1}$ NWs	1.55	3.31	0.1 M $HClO_4$ + 0.2 M Methanol	Nano lett. 2016,16, 5037
RDH PtNi NFs	1.04	1.90		Nano lett. 2016, 16, 2762
Pt_3Cu Nanoctahedra	0.736	2.14		ACS Nano 2015, 9, 7634
PtNi CNCs		1.37	0.5 M H_2SO_4 + 0.5 M Methanol	Adv. Funct. Mater. 2018, 28, 1704774
$Pt_1Cu_1Co_1Ni_1$ 3D NPQA	0.45			ACS Appl. Mater. Interfaces 2016, 8, 6110
Pt–Ru/c-MWNT	1.236	1.4		J. Mater. Chem. A 2015, 3, 8459
G-Cys-Au@Pt	0.674		0.1 M H_2SO_4 + 0.1 M Methanol	Adv. Energy Mater. 2018, 1702609
HTCS $Au_{100}@Pd_{20}Pt_{20}$ NPs	0.64	1.16	0.5 M H_2SO_4 + 1 M Methanol	J. Mater. Chem. A 2017, 5, 18878
np-$Pt_{60}Cu_{40}$	0.75	4.9		ACS Catal. 2015, 5, 3779
Pt–Ni CNCs		1.86	0.5 M H_2SO_4 + 2 M Methanol	Angew. Chem. Int. Ed. 2014, 53, 12522

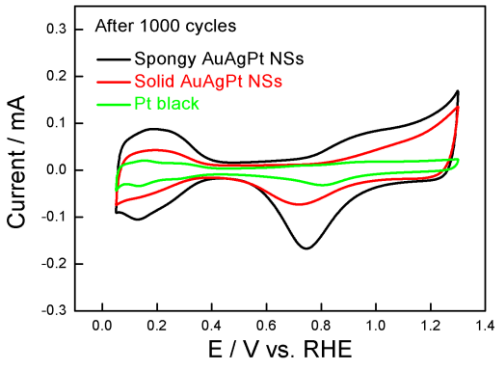

Fig. S10 CV curves for MOR of catalysts (spongy AuAgPt NSs, solid AuAgPt NSs, and Pt black) recorded after 1000 potential cycles**.**

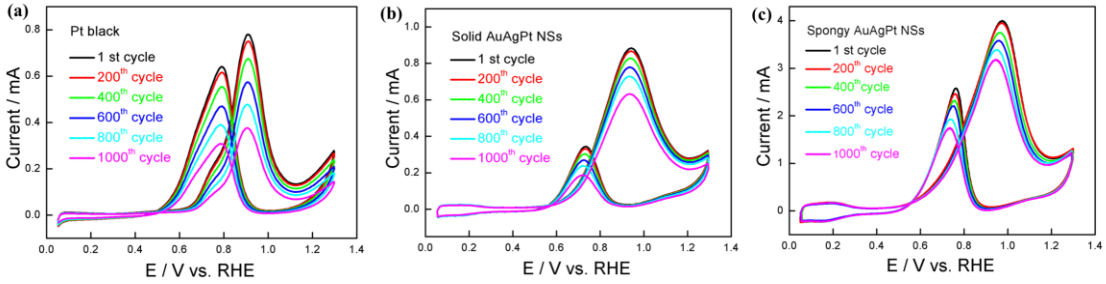

Fig. S11 CV curves (1st, 200th, 400th, 600th, 800th and 1000th cycle) of Pt black (a), solid AuAgPt NSs (b), and spongy AuAgPt NSs (c) for MOR, respectively. Potential was continuously scanned for 1000 sweeping cycles at 50 mV/s in 0.1 M $HClO_4$ + 0.2 M CH_3OH for MOR durability test.

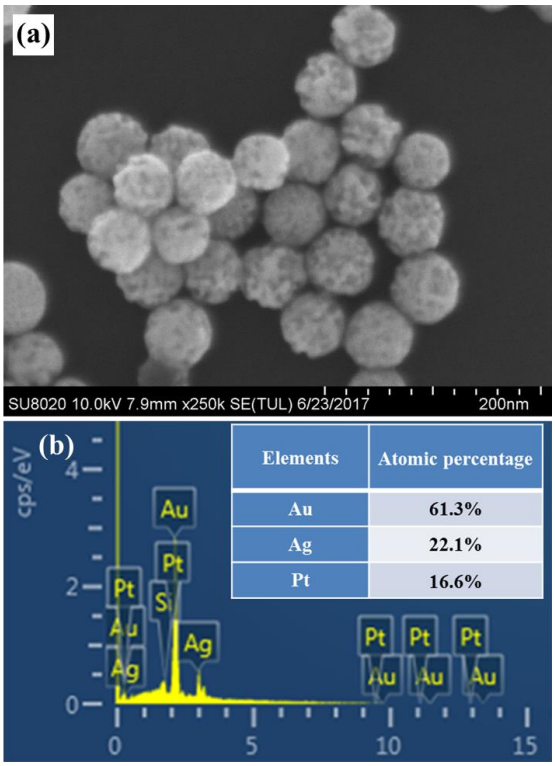

Fig. S12 FESEM (a) and EDS spectrum (b) of spongy AuAgPt NSs after durability test. It can be seen that the spongy structures were well preserved.

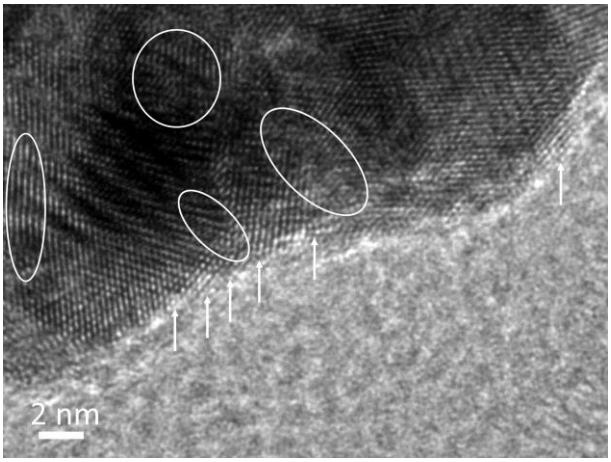

Fig. S13 HRTEM image of spongy AuAgPt NSs after durability test. The grain boundaries, high-index facets and lattice distortion maintained well.

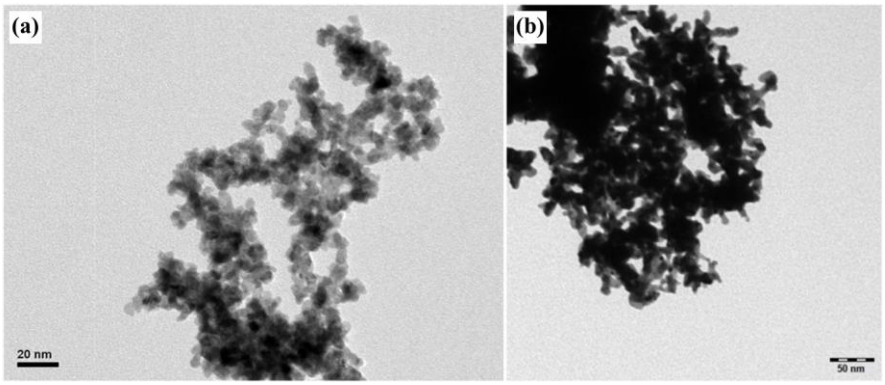

Fig. S14 TEM images of the commercial Pt black before (a) and after (b) durability test.

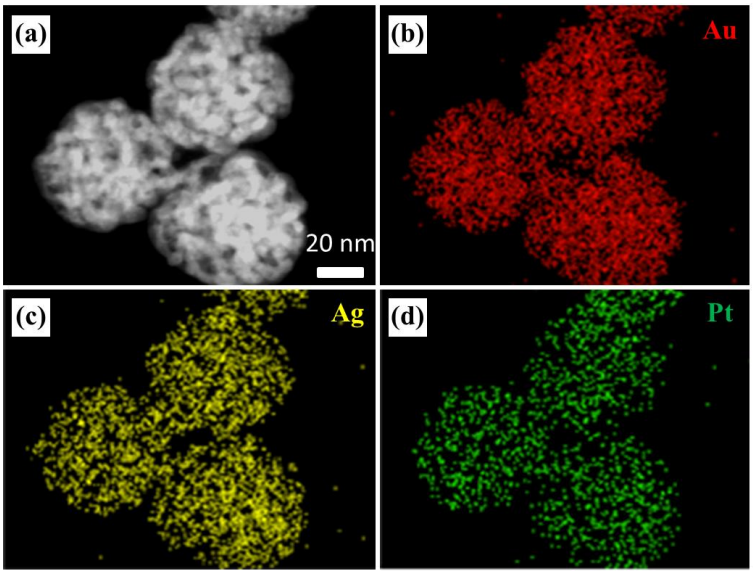

Fig. S15 HAADF-STEM image (a) and EDS elemental mapping (b-d) of spongy AuAgPt NSs without grain boundaries, which obtained through annealing the Au@AgPt@SiO_2 NCs at 800 ^oC under 10% H_2+90% N_2 atmosphere, followed by removing the SiO_2 shell and HNO_3 etching. The percentage of Au, Ag and Pt was 63.2%, 21.1% and 15.7%, respectively, which was similar to that of spongy AuAgPt NSs with high-index facets, grain boundaries, and subtle lattice distortion.

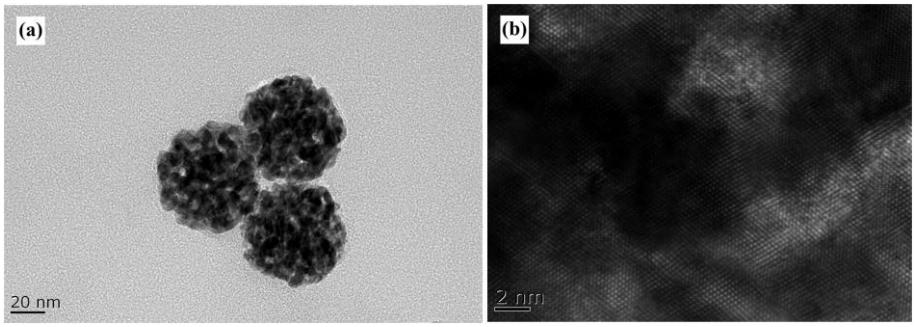

Fig. S16 (a) TEM and (b) HREM images of the spongy AuAgPt NSs, which obtained through annealing the Au@AgPt@SiO_2 NCs at 800 ^oC under 10% H_2+90% N_2 atmosphere, followed by removing the SiO_2 shell and HNO_3 etching. The HRTEM image showed that the grain boundaries were successfully removed.

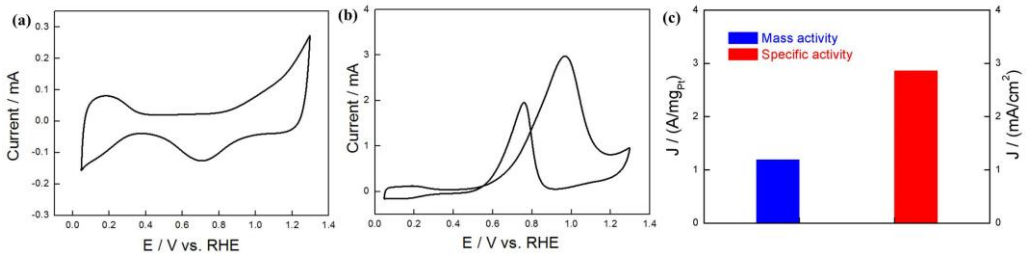

Fig. S17 (a) CV curve, (b) MOR curve, and (c) normalized activities of the spongy AuAgPt NSs without grain boundaries. The CV curve was performed in N_2-saturated 0.1 M $HClO_4$ solution at a scan rate of 50 mV/s and the MOR curve was operated in 0.1 M $HClO_4$ +0.2 M methanol solution at a scan rate of 50 mV/s. The ECSA, mass activity, and specific activity were 41.71 m^2/g, 1.19 A/mg_{pt}, and 2.86 mA cm^{-2}, respectively.

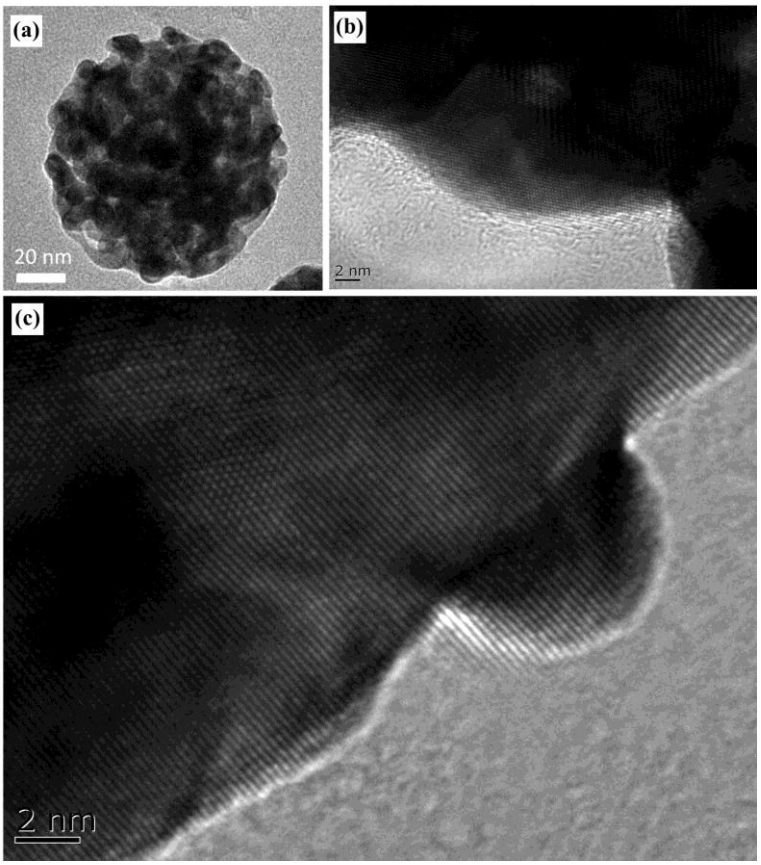

Fig. S18 (a) TEM and (b) HREM images of the spongy AuAgPt NSs annealed at 200 ^{o}C under 10% H_2 + 90% N_2 atmosphere for 1 h. The high-index facets and grain boundaries were successfully removed from the initial spongy AuAgPt NSs.

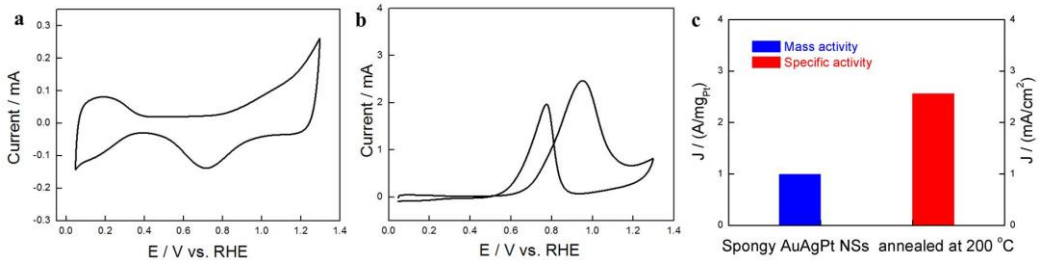

Fig. S19 (a) CV curve, (b) MOR curve, and (c) normalized activities of the spongy AuAgPt NSs without high-index facets and grain boundaries. The ECSA, mass activity, and specific activity were 38.60 m^2/g, 0.99 A/mg_{pt}, and 2.56 mA cm^{-2}, respectively.